ARTICLE

Laser-Synthesized Epitaxial Graphene

Sangwon Lee,[†] Michael F. Toney,[‡] Wonhee Ko,[§,⊥] Jason C. Randel,[§,⊥] Hee Joon Jung,[†] Ko Munakata,[§] Jesse Lu,[¶] Theodore H. Geballe,[§] Malcolm R. Beasley,[§] Robert Sinclair,[†] Hari C. Manoharan,[⊥,#] and Alberto Salleo[†,*]

[†]Department of Materials Science and Engineering, Stanford University, Stanford, California 94305, United States, [‡]Stanford Synchrotron Radiation Lightsource, SLAC National Accelerator Laboratory, Menlo Park, California 94025, United States, [§]Department of Applied Physics, Stanford University, Stanford, California 94305, United States, [⊥]Stanford Institute for Materials and Energy Sciences, SLAC National Accelerator Laboratory, Menlo Park, California 94025, United States, and [¶]Department of Electrical Engineering and [#]Department of Physics, Stanford University, Stanford, California 94305, United States

ABSTRACT Owing to its unique electronic properties, graphene has recently attracted wide attention in both the condensed matter physics and microelectronic device communities. Despite intense interest in this material, an industrially scalable graphene synthesis process remains elusive. Here, we demonstrate a high-throughput, low-temperature, spatially controlled and scalable epitaxial graphene (EG) synthesis technique based on laser-induced surface decomposition of the Si-rich face of a SiC single-crystal. We confirm the formation of EG on SiC as a result of excimer laser irradiation by using reflection high-energy electron diffraction (RHEED), Raman spectroscopy, synchrotron-based X-ray diffraction, transmission electron microscopy (TEM), and scanning tunneling microscopy (STM). Laser fluence controls the thickness of the graphene film down to a single monolayer. Laser-synthesized graphene does not display some of the structural characteristics observed in EG grown by conventional thermal decomposition on SiC (0001), such as Bernal stacking and surface reconstruction of the underlying SiC surface.

KEYWORDS: epitaxial graphene · SiC · synthesis · laser · characterization

Much exciting materials physics centered around graphene has been uncovered in only a few years since the realization that a single-layer graphene sheet is stable.[1−3] Control over the synthesis of this material however is still being developed and high-quality wafer-scale graphene layers cannot be reproducibly fabricated. Various synthesis approaches have been suggested by different research groups.[2,4−12] The first graphene studies were made on micromechanically exfoliated highly oriented pyrolitic graphite.[2] While this method produces high-quality graphene flakes, it is not suitable for scaling and industrial production. More recently, methods based on chemical vapor deposition (CVD) on a transition metal film or surface segregation of carbon out of a supersaturated metal (Ru) film were proposed.[7−10,13] Using these techniques, graphene films were obtained over large areas; however, since the synthesis occurs at high temperature (~1000 °C), the large difference in the thermal expansion coefficients between the materials leads upon cooling to the formation of wrinkles up to tens of nm in height in the graphene layer. Furthermore, the quality of the graphene layer is sensitive to the grain structure of the underlying metal: ultrasmooth essentially single crystalline regions in the metal films are required to obtain good quality graphene. Finally, the graphene films grown on metals must be subsequently transferred to substrates suitable for the fabrication of microelectronic devices. Other graphene preparation methods based on chemical synthesis[6] or unzipping of nanotubes[11,12] suffer from drawbacks such as low yield and difficulty to controllably position the graphene films on a substrate.

A very promising route toward the synthesis of well-controlled and uniform graphene films for electronic applications is thermal decomposition of SiC. By heating SiC in a vacuum, Si evaporates and a layer of graphene forms, termed epitaxial graphene (EG) because of its crystallographic relationship with the underlying SiC lattice.[4,5] EG on SiC has recently been shown to have a nearly ideal graphene band structure,[14] and the fabrication of arrays of electronic devices on EG has already been demonstrated.[15] High decomposition temperature however largely limits this method to single-crystal SiC substrates in ultrahigh vacuum (~1250 °C)[2,16] or inert gas atmospheres (~1650 °C).[17,18] The lowest synthesis temperature reported so far is 950 °C using a carbon deposition method.[19] These high synthesis temperatures coupled with the relatively long growth durations present challenges for materials integration, cost, and synthesis throughput.

Here we report a novel method to synthesize EG on SiC using pulsed KrF laser radiation ($\lambda = 248$ nm, pulse length ≈ 25 ns) in a vacuum attainable within short pump-

*Address correspondence to asalleo@stanford.edu.

Received for review July 27, 2010 and accepted November 23, 2010.

Published online December 1, 2010. 10.1021/nn101796e

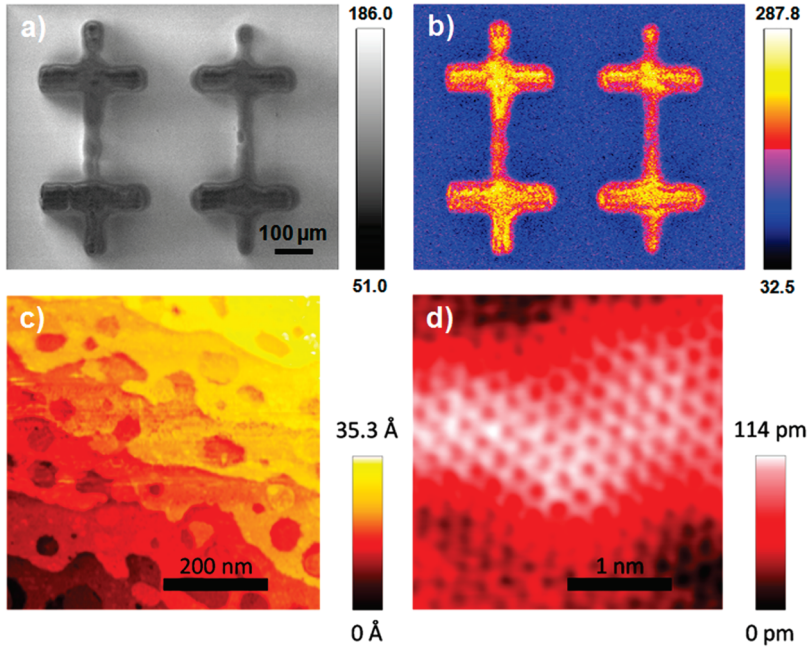

Figure 1. Direct patterning of graphene on SiC using pulsed excimer laser irradiation (a) SEM image (acceleration voltage = 3 keV) of laser-processed SiC with a shadow mask placed in the beampath. (b) Spatial Auger mapping (acceleration voltage = 3 keV) of the intensity of the C (KLL) transition on a laser-processed SiC suface. The laser beam footprint and its spatial modulation are clearly seen. The red and yellow pixels correspond respectively to single and double-layer graphene. (c) STM image of graphene on the surface of 4H-SiC (0001). The surface shows terraces of height 0.3−0.4 nm. (d) Atomic-resolution STM image of a region of the sample characterized in panel c. Bias voltage V_P = 300 mV and the tunneling current I_T = 100 pA for panels c and d. An STM image of a region displaying both single and double-layer graphene is shown in the Supporting Information.

down times in commercial processing tools ($\sim 10^{-6}$ Torr). Under these synthesis conditions, the thermal diffusion length in SiC during the laser pulse ($L_T \approx 4.1$ μm) is much larger than the optical absorption length ($\alpha^{-1} \approx 76$ nm): the laser can thus be considered as a surface heating source on SiC. As a result, the substrate is held essentially at room temperature except for the thin SiC surface layer that absorbs the laser light.[20] This new synthesis technique presents many advantages. Because only the SiC surface is heated, SiC-on-Si could be used as a substrate, which would allow a scaling beyond the 2 inch SiC wafers currently available as well as integration with CMOS electronics. Furthermore, this synthesis process is compatible with conventional microelectronics fabrication. Finally, synthesis and patterning can be done in one step by simply shaping or masking the laser beam.

RESULTS AND DISCUSSION

In initial experiments, n-type (3×10^{18} cm^{-3}) 4H-SiC(0001) chips (5 mm × 5 mm), on-axis, cut from a single crystal wafer were irradiated with a KrF excimer laser beam in a UHV chamber ($P < 10^{-9}$ Torr) equipped with an *in situ* RHEED setup (Supporting Information, Figure S1) to monitor the graphene formation process. Irradiation was performed at ~1.2 J/cm^2 average fluence on a 2 mm^2 spot size (3.25 mm × 0.625 mm) over a 25 mm^2 area of the sample for 500 pulses. The SiC was oriented in the [10$\bar{1}$0] azimuth in the electron beam and consequently the SiC (2$\bar{1}$) RHEED streaks were observed. After irradiation, two new RHEED streaks appeared corresponding to a plane (*d*) spacing of 1.23 Å, which matches the (1$\bar{1}$) reflections of graphite, as expected from the epitaxial relationship of the graphite lattice with respect to the underlying SiC substrate (Supporting Information, Figure S1).[21,22] After these results, a second set of experiments was conducted in a non-UHV chamber ($P \approx 10^{-6}$ Torr) with the goal of confirming the formation of graphene and determining its thickness, structural quality, and uniformity by using a range of complementary analytical techniques.

To demonstrate the ability to pattern EG during synthesis, a shadow-mask was placed in the laser beam path. A focusing lens was also used to reduce the beam size by 5× (Figure 1a). Occasionally a visible luminescence was observed upon laser irradiation but we did not study its spectral or temporal characteristics. Surface compositional mapping using scanning auger electron spectroscopy (s-AES) confirmed that the carbon concentration at the surface of SiC in the laser-irradiated regions was higher than in the rest of the substrate (Figure 1b). The thickness of the carbon-rich regions was estimated using the ratio of the Si (LVV, E = 92 eV) to C (KLL, E = 271 eV) peak areas.[5,16,21] Surface enrichment of C equivalent to a monolayer or a bilayer only were observed (Supporting Information, Figure S2). Scanning tunneling microscopy (STM) was used to

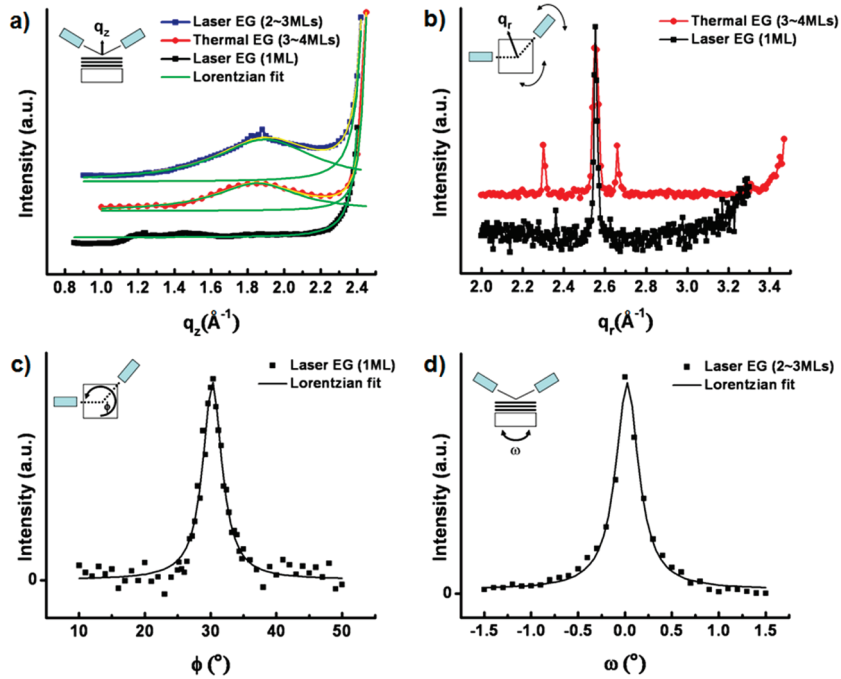

Figure 2. Synchrotron X-ray diffraction of laser-synthesized and thermally grown epitaxial graphene (EG). (a) Specular scan, (b) radial scan across the (10) rod of EG, revealing that a peak located at the q_r expected for the (10) rod (2.55 Å^{-1}). The peaks located at 2.37 and 2.67 Å^{-1} are SiC surface reconstruction peaks. The plots are offset for clarity. (c) Azimuthal phi-scan of the (100) in-plane peak of laser-synthesized EG (sample B). The off-peak signal is equal to the baseline indicating that there is no randomly oriented graphene on the SiC substrate. (d) Rocking scan about the (0002) peak of laser-synthesized EG (sample A).

confirm that the C-rich regions of the surface were indeed graphene. The surface of the laser-processed regions was smooth with large terraces 5.5 ± 0.5 Å high (Figure 1c), consistent with twice the distance between subsurface Si planes in SiC (0001) (2.52 Å). We also observe 3.5 ± 0.5 Å steps around smaller features, consistent with expected graphene layer thickness (3.40 Å).[23−26] We conclude that these steps constitute the boundaries between regions of graphene with different number of layers. Atomic-resolution STM on the smooth regions of the film displayed a honeycomb symmetry, a signature of single-layer graphene (Figure 1d).[26−28] The lattice constant measured from the topograph in Figure 1d is 2.2 ± 0.2 Å, consistent with the expected graphene lattice constant (2.46 Å). From a large atomic-resolution topograph, we confirmed that this single layer of graphene extends continuously over more than a 10 nm × 10 nm area. Notably, no periodic surface reconstruction of SiC (0001) was observed (Supporting Information, Figure S3), which is a common feature of thermally grown EG on SiC (0001).

Additional structural characterization of laser-synthesized EG was performed with X-ray diffraction at the Stanford Synchrotron Radiation Lightsource (SSRL). On similar SiC substrates, a film of thermally grown EG was used as a reference, where an average thickness of 5 ± 2 layers had been measured *in situ* at the end of the growth by X-ray photoelectron spectroscopy (XPS).[18,29] A specular scan of the thermally grown EG displayed a broad peak centered at q_z = 1.85 Å^{-1}, with a fwhm =0.55 Å^{-1} (Figure 2a) corresponding to a ~1.1 nm thick (3−4 layers) graphene film, in agreement with the XPS data. Two films of laser-synthesized EG were studied. Sample A was made using 500 1.2 J/cm^2 pulses at 20 Hz; sample B was made using 500 1 J/cm^2 pulses at 20 Hz. Sample A displayed a broad peak (q_z = 1.89 Å^{-1}, fwhm = 0.66 Å^{-1}) corresponding to an average of two to three graphene layers in agreement with a separate estimate obtained by s-AES on the same film. The *d*-spacing of the laser-synthesized EG film ($d \approx 3.32$ Å) is close to that of thermally grown EG ($d \approx 3.40$ Å) and bulk graphite (d = 3.35 Å). No specular diffraction peak was observed in sample B (Figure 2a). High-resolution grazing incidence X-ray diffraction was used to study the structure of the EG in the film plane (Figure 2b). Sample B displayed the typical features of the graphene unit cell as shown in a radial scan along the (10) direction of the graphene lattice (q_r = 2.55 Å^{-1}, a_G = 2.46 Å).[30,31] Because of the lack of specular diffraction, we conclude that sample B is a graphene monolayer over the area sampled by the X-ray beam. An L-scan (*i.e.*, out-of-plane scan) of this peak in sample A (data not shown) had no intensity oscillations, suggesting that the graphene layers are not Bernal-stacked. The in-plane crystalline coherence length in sample B was ~40 nm, as determined by the fwhm of the

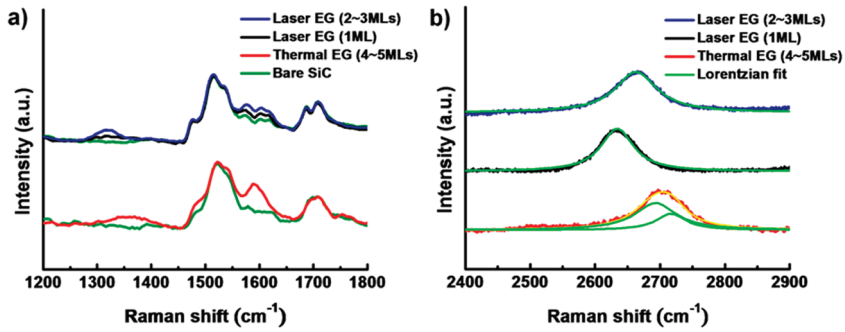

Figure 3. Raman spectra of laser-synthesized EG and thermally grown EG. (a) D and G Raman peaks of mono- (black trace), bi-, or trilayer (blue trace) and many-layer graphene (red trace). The Raman spectrum of the 4H-SiC(0001) substrate is included (green trace). The SiC substrates are different (see Experimental Section), hence the differences in the Raman spectra of the bare substrates. (b) 2D Raman peak of laser-synthesized EG (blue and black traces) and thermally grown EG (red). Curve fitting of the 2D peak using a single Lorentzian for laser-synthesized EG and multiple Lorentzians for thermally grown EG (yellow line). The data is normalized to the maximum peak height.

diffraction peak in the radial direction (fwhm = 0.017 $Å^{-1}$). This figure may seem small but it should be emphasized that it must not be compared to "domain sizes" or characteristic length scales extracted using other techniques (*e.g.*, low-energy electron microscopy). Indeed, these other techniques are not sensitive to atomic disorder and overestimate the grain-sizes, whereas terraces may be composed of multiple subdomains with smaller crystalline coherence length.[32] In fact, comparable in-plane coherence length (~25 nm) was obtained for the reference thermally grown EG film, in agreement with previously reported graphene grain-sizes measured by X-ray diffraction on SiC(0001).[33] We conclude that the structural coherence length is most likely limited by the initial SiC surface quality[18,30] and not by the synthesis process. Interestingly, the SiC reconstruction peaks (q_r = 2.37 $Å^{-1}$ and q_r = 2.67 $Å^{-1}$) were not observed in laser-synthesized EG while they appeared in thermally grown EG (Figure 2b) and have also been reported previously.[23,33] Thus the interface layer between the SiC substrate and the laser-synthesized EG film has a different structure than that of thermal EG.[21,30] Because the SiC−graphene interface affects the electrical properties of EG such as bandgap and doping,[34,35] the absence of surface reconstruction could have important implications for the electronic properties of the film. An azimuthal (phi) scan of the in-plane (100) peak was used to verify the in-plane texture of laser-synthesized EG (Figure 2c). The substrate was oriented with phi = 0° along the [10$\bar{1}$0] direction of SiC. The absolute angle (30°) with respect to the underlying SiC lattice and the narrow fwhm (=3.5°) of the diffracted intensity confirmed that laser-synthesized EG was epitaxial and displayed the expected crystallographic relationship with the SiC substrate. Finally, the quality of the out-of-plane texture of laser-synthesized multilayer EG (sample A) was measured using a rocking scan about the (0002) peak (Figure 2d). The film had only a small angular misorientation range (fwhm = 0.30°) relative to the substrate normal, comparable to that of thermally grown EG (Supporting Information, Figure S4).

Raman spectroscopy provides a semiquantitative way of characterizing the thickness and structural quality of graphene layers.[1,36] We carried out Raman measurements on the same films as those used for X-ray diffraction using thermally grown EG as a reference (Figure 3). The features of Raman spectra are sensitive to the bonding and stress between the substrate and the EG layer.[37,38] In laser-synthesized EG however there is no surface reconstruction of the underlying SiC substrate and the stress state of the EG film is likely different from that of thermally grown EG. Therefore, Raman spectra of laser-synthesized EG should not necessarily be identical to that of thermally grown EG (Figure 3a).[18,38] Nevertheless, the G and 2D peaks were clearly visible in the differential spectra obtained by subtracting the Raman spectrum of the bare SiC sample from that of the graphitized samples (Supporting Information, Figure S5). The D peak is due to defects and disorder while the G band is the symmetry-allowed graphite band. The graphene peaks were located in the spectral regions (near ~1350 and ~1580 cm^{-1} for the D and G peaks, respectively) where they have been previously reported.[36−41] The presence and intensity of the D peak are consistent with the relatively short coherence length measured by X-ray diffraction and suggest the presence of edge-termination defects in the EG films. The second order of the D peak (2D peak) is related to the thickness and electronic properties of graphene.[36] The wavenumber of the 2D peak in laser-synthesized graphene increased from ~2635 to ~2665 cm^{-1} as the layer number increased from 1 to 2−3 (Figure 3b). This tendency of the 2D peak to shift to higher energy with thickness has been observed in thermally grown EG before.[37,42] The 2D peak of laser-synthesized EG was fitted with a single

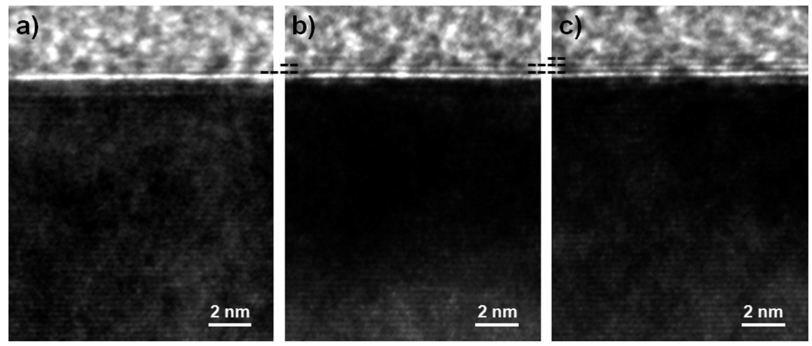

Figure 4. HRTEM images of graphene layers on 4H-SiC (0001) on-axis surface. Film thickness measurements are confirmed *via* TEM. (Acceleration voltage = 200 kV) Dashed lines denote (a) a single graphene layer, (b) two graphene layers, and (c) three graphene layers. Micrographs are taken in the [10$\bar{1}$0] SiC sample orientation.

Lorentzian having a fwhm of ~60 cm^{-1} for monolayer EG and ~75 cm^{-1} for 2−3 layer EG. The 2D peak of thermal EG on the other hand was fitted by multiple Lorentzians, in agreement with previous reports. Single-peak fitting of the 2D peak has been observed in multilayer thermally grown EG on the C-rich SiC face and is a sign of electronic decoupling between the graphene layers. This effect is responsible for monolayer graphene-like properties of multilayer EG.[39,43] Thus, Raman spectroscopy suggests that the graphene layers in laser-synthesized multilayer EG are not Bernal-stacked, in agreement with the X-ray L-scans, and therefore they may be electronically decoupled, a feature not observed before in EG grown on Si-terminated SiC. Electronic decoupling of the EG layers relaxes the requirement that EG be a monolayer to exhibit graphene-like electronic properties.[5,30,39]

Finally, high-resolution TEM (HRTEM) micrographs taken along the [10$\bar{1}$0] zone axis of SiC confirmed the presence of EG (Figure 4). Micrographs were taken on three different EG films made in increasing order of laser fluence (~1.1, ~1.2, and ~1.4 J/cm^2 with 500 pulses, panels a to c), which led to thicker graphene layers. The measured interlayer distance (3.31 ± 0.04 Å) agrees with the interplanar spacing of graphite (d = 3.35 Å) and the X-ray diffraction measurements.

All our characterization data confirm that laser-irradiation of SiC (0001) leads to the formation of EG, which can be as thin as a monolayer over large areas. The fluence of the laser pulse controls the thickness of the EG layer with nearly single-layer accuracy. We find that laser-synthesized EG on the Si-terminated face is of equal structural quality as graphene grown thermally in UHV on the same substrate. While higher-quality films have been recently grown in an Ar atmosphere,[17,18] ours is the first report of laser-based synthesis of graphene. The quality of thermally grown graphene has been continuously improved in the last 8 years by fine-tuning the synthesis process. Consequently, we surmise that there is also much room to improve our laser-based process and there is no fundamental obstacle to the synthesis of higher-quality material.

Laser irradiation certainly heats-up the SiC surface; however, a simple estimate demonstrates that the EG formation mechanism is not exclusively thermal decomposition but is consistent with a photophysical component often observed in UV laser processing of transparent dielectrics.[44] To form a graphene monolayer, approximately 0.37 Si atoms/$Å^2$ must sublime away. The maximum Si effusion rate during the pulse can be calculated using the Hertz−Knudsen−Langmuir equation (see Supporting Information). During the irradiation with a 1 J/cm^2 pulse lasting 25 ns, approximately 10^{-9} Si atoms/$Å^2$ sublime away. Therefore, even after 500 pulses the total amount of thermally sublimed Si is much smaller than that needed to form a graphene monolayer. Even if the surface reached the melting point of SiC (~2700 °C)—which is highly unlikely since we find no evidence of melting by SEM analysis - the amount of sublimed Si during the 500 pulses is only ~10^{-2} atoms/$Å^2$. These estimates strongly suggest that the thermal effusion flux is not sufficient to cause the formation of an EG layer in our irradiation conditions. We hypothesize that the EG forms during a strongly out-of-equilibrium process where the high-energy (5 eV) photons promote photophysical Si−C bond cleaving and allow the Si evaporation rate at the SiC surface to exceed the equilibrium effusion flux at any given temperature. The photophysical formation mechanism we postulate here is fundamentally different from thermal processes previously observed in laser-irradiation of SiC.[45,46]

CONCLUSION

We developed an alternative room-temperature technique to synthesize EG on SiC that is scalable, does not need UHV, and can be integrated with other fabrication technologies. Laser-synthesis of EG allows the synthesis and patterning of graphene in one single fabrication step and could be used for rapid prototyping of devices. The structural quality

of the EG made by laser-synthesis on SiC (0001) is similar to that of thermally grown EG on SiC (0001). There are however significant differences between the two materials as no surface reconstruction of the SiC surface is observed in laser-synthesized EG. Furthermore, multilayer EG synthesized with the laser is not Bernal-stacked strongly suggesting electronic decoupling between the layers.

EXPERIMENTAL SECTION

Sample Preparation (Laser Synthesis of Epitaxial Graphene on SiC). N-type (nitrogen, 3×10^{18} cm^{-3}) 4H-SiC(0001) wafer, on-axis, with chemical mechanical polishing (CMP, Ra $\leq$ 1 nm) on the Si face was purchased from SiCrystal AG, which was used for RHEED, X-ray diffraction, and TEM characterizations. High-purity semi-insulating ($\rho \geq 1 \times 10^5$ $\Omega \cdot cm$) 4H-SiC(0001) wafer, on-axis, was also purchased from Cree: the wafer was epiready polished by NovaSiC up to an atomically flat surface (Rq $\leq$ 1 Å), which was used for STM and Raman measurements. The substrates (5 mm $\times$ 5 mm) were cut from the wafers and treated by sequential ultrasonic bath in acetone, methanol, and isopropyl alcohol (for 5 min to remove grease), Piranha cleaning (mixture of H_2SO_4 + H_2O_2 (1:1) for 3 min to wipe off metal powder and organic contaminants) and HF etching (10% HF solution for 3 min to remove the surface oxide). The sample was placed in a high-vacuum (HV) chamber (base pressure $\approx 10^{-7}$ Torr, pumpdown time $\approx$ 2 h) designed for pulsed laser deposition (PLD). The SiC surface was irradiated with a pulsed KrF excimer laser (Lambda Physik LPX 210i, $\lambda = 248$ nm, pulse length $\approx$ 25 ns) with a nonhomogenized beam. The beam intensity profile was measured with 1 mm interval at the removable beam blocker with hole (20 mm $\times$ 10 mm) near the laser exit port, and the regions with higher fluence than average were blocked by shadow mask (stainless steel). The SiC substrate with specially designed holder was loaded, inside the chamber, perpendicular in the direction of the laser beam. The experiments were performed at $\sim$1.1, $\sim$1.2, and $\sim$1.4 J/cm^2 with 500 shots (20 Hz, 25 s) to synthesize monolayer, bilayer, trilayer graphene, respectively. The vacuum condition of $\sim 10^{-6}$ Torr was used for all experiments.

Sample Preparation (Thermal Growth of Epitaxial Graphene on SiC). The substrates (5 mm $\times$ 5 mm) were cut from the same wafer (N-type) used for the laser-synthesized EGs and treated by sequential ultrasonic bath in acetone and methanol. The sample was placed in an ultrahigh vacuum (UHV) chamber (base pressure $\approx 10^{-9}$ Torr, pumpdown time $\approx$ 10 h) equipped with an *in situ* XPS and RHEED setup. The sample was first heated up to $\sim$800 °C and Si was evaporated to remove the surface oxide. The sample was then heated up to 1400$-$1500 °C depending on the number of graphene layers.

Scanning Tunneling Microscopy (STM). STM data were acquired by low-temperature ultrahigh-vacuum (UHV) STM with base pressure $< 3 \times 10^{-11}$ Torr and measurement temperature of 77 K. After loading into UHV, the graphene sample was heated up to 800 °C for a few hours in the UHV chamber. The pressure was kept below 2.5×10^{-8} Torr during this outgassing procedure. The STM tip (polycrystalline Pt/Ir) was prepared by *in situ* field emission over an atomically clean Ag(111) surface prepared by repeated cycles of Ar sputtering and annealing. The tip condition was verified by inspecting topography and spectroscopy on Ag(111) before switching to the graphene sample. The Ag(111) crystal also served as a reference for calibration.

Grazing Incidence X-ray Diffraction (GIXD). GIXD experiments were performed at the Stanford Synchrotron Radiation Lightsource (SSRL) on Beamline 7-2. The experiments were conducted at ambient conditions with an X-ray energy of 8 keV and an incidence angle just above the SiC critical angle (about 0.4 degrees). The diffracted beam was collimated with 1 millradian Soller slits and detected with a Vortex detector.

Raman characterization. Micro-Raman measurements were performed at room temperature on both laser-synthesized EG and thermally grown EG samples. A LabRam Aramis (Horiba Jobin Yvon) microscope equipped with a $\times$100 objective was used. The excitation source was a 633 nm HeNe laser (spot size, $\sim$1 μm) with a power of 5 mW, taking special care to avoid surface heating. The integration time was 10 s (Figure 3a) and 15 s (Figure 3b) at each spot.

Transmission Electron Microscopy (TEM). TEM samples were prepared using a focused ion beam (FIB, FEI Strata 235DB dual-beam FIB/SEM) lift-out technique. Prior to ion milling, the samples were protected with amorphous carbon paint as a capping layer to preserve the initial surface integrity. The samples were then prepared by FIB milling with a Ga ion beam at 30 keV to a thickness of $\sim$80 nm. Then the samples transferred to a Cu TEM grid with Omniprobe were inserted into and FEI CM20 TEM operated at an accelerating voltage of 200 kV. After finding the [10$\bar{1}$0] zone axis of SiC using its diffraction pattern (data not shown), cross-sectional observations of the interface between graphene and SiC, bright-field TEM images, were taken for three of the samples.

Acknowledgment. A.S. gratefully acknowledges support from the Center for Integrated Systems at Stanford (seed program), NSF-CMMI-0926212 and Electro Scientific Industries. Portions of this research were carried out at the Stanford Synchrotron Radiation Lightsource, a national user facility operated by Stanford University on behalf of the U.S. Department of Energy, Office of Basic Energy Sciences. H.C.M., W.K., and J.R. are supported by the Department of Energy, Office of Basic Energy Sciences, Division of Materials Sciences and Engineering, under contract DE-AC02-76SF00515. Probe development and measurement supported by the NSF-DMR. Helpful conversations with Prof. Goldhaber-Gordon are gratefully acknowledged as well.

Supporting Information Available: Calculation of the Si thermal effusion rate, Figure S1$-$S5. This material is available free of charge *via* the Internet at http://pubs.acs.org.

REFERENCES AND NOTES

1. Geim, A. K.; Novoselov, K. S. The Rise of Graphene. *Nat. Mater.* **2007**, *6*, 183–191.
2. Novoselov, K. S.; Geim, A. K.; Morozov, S. V.; Jiang, D.; Zhang, Y.; Dubonos, S. V.; Grigorieva, I. V.; Firsov, A. A. Electric Field Effect in Atomically Thin Carbon Films. *Science* **2004**, *306*, 666–669.
3. Geim, A. K. Graphene: Status and Prospects. *Science* **2009**, *324*, 1530–1534.
4. Badami, D. V. Graphitization of α-Silicon Carbide. *Nature* **1962**, *193*, 569–570.
5. Berger, C.; Song, Z. M.; Li, X. B.; Wu, X. S.; Brown, N.; Naud, C.; Mayou, D.; Li, T. B.; Hass, J.; Marchenkov, A. N.; *et al.* Electronic Confinement and Coherence in Patterned Epitaxial Graphene. *Science* **2006**, *312*, 1191–1196.
6. Li, X. L.; Wang, X. R.; Zhang, L.; Lee, S.; Dai, H. J. Chemcally Derived, Ultrasmooth Graphene Nanoribbon Semiconductors. *Science* **2008**, *319*, 1229–1232.
7. Sutter, P. W.; Flege, J. I.; Sutter, E. A. Epitaxial Graphene on Ruthenium. *Nat. Mater.* **2008**, *7*, 406–411.
8. Karu, A. E.; Beer, M. Pyrolytic Formation of Highly Crystalline Graphite Films. *J. Appl. Phys.* **1966**, *37*, 2179–2181.
9. Kim, K. S.; Zhao, Y.; Jang, H.; Lee, S. Y.; Kim, J. M.; Kim, K. S.; Ahn, J. H.; Kim, P.; Choi, J. Y.; Hong, B. H. Large-Scale Pattern Growth of Graphene Films for Stretchable Transparent Electrodes. *Nature* **2009**, *457*, 706–710.
10. Li, X.; Cai, W.; An, J.; Kim, S.; Nah, J.; Yang, D.; Piner, R.; Velamakanni, A.; Jung, I.; Tutuc, E.; *et al.* Large-Area Synthesis of High-Quality and Uniform Graphene Films on Copper Foils. *Science* **2009**, *324*, 1312–1314.

11. Kosynkin, D. V.; Higginbotham, A. L.; Sinitskii, A.; Lomeda, J. R.; Dimiev, A.; Price, B. K.; Tour, J. M. Longitudinal Unzipping of Carbon Nanotubes to Form Graphene Nanoribbons. *Nature* **2009**, *458*, 872–876.
12. Jiao, L.; Zhang, L.; Wang, X.; Diankov, G.; Dai, H. Narrow Graphene Nanoribbons from Carbon Nanotubes. *Nature* **2009**, *458*, 877–880.
13. Reina, A.; Jia, X.; Ho, J.; Nezich, D.; Son, H.; Bulovic, V.; Dresselhaus, M. S.; Kong, J. Large Area, Few-Layer Graphene Films on Arbitrary Substrates by Chemical Vapor Deposition. *Nano Lett.* **2009**, *9*, 30–35.
14. Sprinkle, M.; Siegel, D.; Hu, Y.; Hicks, J.; Tejeda, A.; Taleb-Ibrahimi, A.; Le Fèvre, P.; Bertran, F.; Vizzini, S.; Enriquez, H.; *et al*. First Direct Observation of a Nearly Ideal Graphene Band Structure. *Phys. Rev. Lett.* **2009**, *103*, 226803.
15. Kedzierski, J.; Hsu, P.-L.; Healey, P.; Wyatt, P. W.; Keast, C. L.; Sprinkle, M.; Berger, C.; de Heer, W. A. Epitaxial Graphene Transistors on SiC Substrates. *IEEE Trans. Electron Devices* **2008**, *55*, 2078–2085.
16. Berger, C.; Song, Z.; Li, T.; Li, X.; Ogbazghi, A. Y.; Feng, R.; Dai, Z.; Marchenkov, A. N.; Conrad, E. H.; First, P. N.; *et al*. Ultrathin Epitaxial Graphite: 2D Electron Gas Properties and a Route toward Graphene-Based Nanoelectronics. *J. Phys. Chem. B* **2004**, *108*, 19912–19916.
17. Virojanadara, C.; Syväjarvi, M.; Yakimova, R.; Johansson, L. I.; Zakharov, A. A.; Balasubramanian, T. Homogeneous Large-Area Graphene Layer Growth on 6H-SiC(0001). *Phys. Rev. B* **2008**, *78*, 245403.
18. Emtsev, K. V.; Bostwick, A.; Horn, K.; Jobst, J.; Kellogg, G. L.; Ley, L.; McChesney, J. L.; Ohta, T.; Reshanov, S. A.; Röhrl, J.; *et al*. Towards Wafer-Size Graphene Layers by Atmospheric Pressure Graphitization of Silicon Carbide. *Nat. Mater.* **2009**, *8*, 203–207.
19. Al-Temimy, A.; Riedl, C.; Starke, U. Low Temperature Growth of Epitaxial Graphene on SiC Induced by Carbon Evaporation. *Appl. Phys. Lett.* **2009**, *95*, 231907.
20. Ohring, M. *The Materials Science of Thin Films*; Academic Press: San Diego, CA, 1992; pp 595−601.
21. Luxmi; Nie, S.; Fisher, P. J.; Feenstra, R. M.; Gu, G.; Sun, Y. Temperature Dependence of Epitaxial Graphene Formation on SiC(0001). *J. Electron. Mater.* **2009**, *38*, 718–724.
22. Lebedev, A. A.; Kotousova, I. S.; Lavrent'ev, A. A.; Lebedev, S. P.; Makarenko, I. V.; Petrov, V. N.; Titkov, A. N. Formation of Nanocarbon Films on the SiC Surface through Sublimation in Vacuum. *Phys. Solid State* **2009**, *51*, 829–832.
23. Hass, J.; Feng, R.; Millán-Otoya, J. E.; Li, X.; Sprinkle, M.; First, P. N.; de Heer, W. A.; Conrad, E. H.; Berger, C. Structural Properties of the Multilayer Graphene/ 4H-SiC(0001□) System As Determined by Surface X-ray Diffraction. *Phys. Rev. B* **2007**, *75*, 214109.
24. Hass, J.; Millán-Otoya, J. E.; First, P. N.; Conrad, E. H. Interface Structure of Epitaxial Graphene Grown on 4H-SiC(0001). *Phys. Rev. B* **2008**, *78*, 205424.
25. Hupalo, M.; Conrad, E. H.; Tringides, M. C. Growth Mechanism for Epitaxial Graphene on Vicinal 6*H*-SiC(0001) Surfaces: A Scanning Tunneling Microscopy Study. *Phys. Rev. B* **2009**, *80*, 041401(R).
26. Rutter, G. M.; Guisinger, N. P.; Crain, J. N.; Jarvis, E. A. A.; Stiles, M. D.; Li, T.; First, P. N.; Stroscio, J. A. Imaging the Interface of Epitaxial Graphene with Silicon Carbide *via* Scanning Tunneling Microscopy. *Phys. Rev. B* **2007**, *76*, 235416.
27. Mallet, P.; Varchon, F.; Naud, C.; Magaud, L.; Berger, C.; Veuillen, J.-Y. Electron States of Mono- and Bilayer Graphene on SiC Probed by Scanning-Tunneling Microscopy. *Phys. Rev. B* **2007**, *76*, 041403(R).
28. Brar, V. W.; Zhang, Y.; Yayon, Y.; Ohta, T.; McChesney, J. L.; Bostwick, A.; Rotenberg, E.; Horn, K.; Crommie, M. F. Scanning Tunneling Spectroscopy of Inhomogeneous Electronic Structure in Monolayer and Bilayer Graphene on SiC. *Appl. Phys. Lett.* **2007**, *91*, 122102.
29. Emtsev, K. V.; Speck, F.; Seyller, Th.; Ley, L.; Riley, J. D. Interaction, Growth, and Ordering of Epitaxial Graphene on SiC{0001} Surfaces: A Comparative Photoelectron Spectroscopy Study. *Phys. Rev. B* **2008**, *77*, 155303.
30. Hass, J.; Varchon, F.; Millán-Otoya, J. E.; Sprinkle, M.; Sharma, N.; de Heer, W. A.; Berger, C.; First, P. N.; Magaud, L.; Conrad, E. H. Why Multilayer Graphene on 4H-SiC(0001□) Behaves Like a Single Sheet of Graphene. *Phys. Rev. Lett.* **2008**, *100*, 125504.
31. Baskin, Y.; Meyer, L. Lattice Constants of Graphite at Low Temperatures. *Phys. Rev.* **1955**, *100*, 544.
32. Snyder, R. L.; Fiala, J.; Bunge, H. J. *Defect and Microstructure Analysis by Diffraction*; Oxford University Press: Oxford, 1999.
33. Charrier, A.; Coati, A.; Argunova, T.; Thibaudau, F.; Garreau, Y.; Pinchaux, R.; Forbeaux, I.; Debever, J.-M.; Sauvage-Simkin, M.; Themlin, J.-M. Solid-State Decomposition of Silicon Carbide for Growing Ultra-Thin Heteroepitaxial Graphite Films. *J. Appl. Phys.* **2002**, *92*, 2479–2484.
34. Zhou, S. Y.; Gweon, G.-H.; Fedorov, A. V.; First, P. N.; de Heer, W. A.; Lee, D.-H.; Guinea, F.; Castro Neto, A. H.; Lanzara, A. Substrate-Induced Bandgap Opening in Epitaxial Graphene. *Nat. Mater.* **2007**, *6*, 770–775.
35. Siegel, D. A.; Zhou, S. Y.; El Gabaly, F.; Fedorov, A. V.; Schmid, A. K.; Lanzara, A. Self-Doping Effects in Epitaxially Grown Graphene. *Appl. Phys. Lett.* **2008**, *93*, 243119.
36. Ferrari, A. C.; Meyer, J. C.; Scardaci, V.; Casiraghi, C.; Lazzeri, M.; Mauri, F.; Piscanec, S.; Jiang, D.; Novoselov, K. S.; Roth, S.; *et al*. Raman Spectrum of Graphene and Graphene Layers. *Phys. Rev. Lett.* **2006**, *97*, 187401.
37. Ni, Z. H.; Chen, W.; Fan, X. F.; Kuo, J. L.; Yu, T.; Wee, A. T. S.; Shen, Z. X. Raman Spectroscopy of Epitaxial Graphene on a SiC Substrate. *Phys. Rev. B* **2008**, *77*, 115416.
38. Röhrl, J.; Hundhausen, M.; Emtsev, K. V.; Seyller, Th.; Graupner, R.; Ley, L. Raman Spectra of Epitaxial Graphene on SiC(0001). *Appl. Phys. Lett.* **2008**, *92*, 201918.
39. Faugeras, C.; Nerrière, A.; Potemski, M.; Mahmood, A.; Dujardin, E.; Berger, C.; de Heer, W. A. Few-Layer Graphene on SiC, Pyrolitic Graphite, and Graphene: A Raman Scattering Study. *Appl. Phys. Lett.* **2008**, *92*, 011914.
40. Tuinstra, F.; Koenig, J. L. Raman Spectrum of Graphite. *J. Chem. Phys.* **1970**, *53*, 1126–1130.
41. Ferrari, A. C.; Robertson, J. Interpretation of Raman Spectra of Disordered and Amorphous Carbon. *Phys. Rev. B* **2000**, *61*, 14095–14107.
42. Lee, D. S.; Riedl, C.; Krauss, B.; von Klitzing, K.; Starke, U.; Smet, J. H. Raman Spectra of Epitaxial Graphene on SiC and of Epitaxial Graphene Transferred to SiO_2. *Nano Lett.* **2008**, *8*, 4320–4325.
43. Lespade, P.; Marchand, A.; Couzi, M.; Cruege, F. Caracterisation de Materiaux Carbones par Microspectrometrie Raman. *Carbon* **1984**, *22*, 375–385.
44. Bäuerle, D. *Laser Processing and Chemistry*; Springer: Berlin, 2000.
45. Ohkawara, Y.; Shinada, T.; Fukada, Y.; Ohshio, S.; Saitoh, H.; Hiraga, H. Synthesis of Graphite Using Laser Decomposition of SiC. *J. Mater. Sci.* **2003**, *38*, 2447–2453.
46. Perrone, D.; Maccioni, G.; Chiolerio, A.; Martinez de Marigorta, C.; Naretto, M.; Pandolfi, P.; Martino, P.; Ricciardi, C.; Chiodoni, A.; Celasco, E.; *et al*. Study on the Possibility of Graphene Growth on 4H-Silicon Carbide Surfaces *via* Laser Processing. Proceedings of the 5th International WLT-Conference on Lasers in Manufacturing, Munich, June, 2009.